# Decentralized Stochastic Disturbance Observer-Based Optimal Frequency Control Method for Interconnected Power Systems With High Renewable Shares

Hassan Haes Alhelou, *Senior Member, IEEE*, Harish Parthasarathy, *Senior Member, IEEE*, Neelu Nagpal, *Senior Member, IEEE*, Vijyant Agarwal, *Member, IEEE*, Hardik Nagpal, and Pierluigi Siano, *Senior Member, IEEE*

***Abstract*—This article proposes a novel, disturbance observer-based decentralized frequency control method for interconnected power systems. The method employs extended Kalman filter (EKF) as an observer to estimate inaccessible dynamic states of the system, including the total disturbance as one of the state variables. An optimal decentralized disturbance observer based controller is suggested for multiarea power systems that compensates the estimated disturbance and further based on minimizing the joint error energies of state estimation error and state tracking error provides its value to the controller for regulating the frequency variation. The proposed method is mathematically designed to be robust against parametric and nonparametric uncertainties. The efficacy and accuracy of the proposed control method is verified considering different types of practical operation scenarios. The results confirm the brilliant and superiority of the proposed method in controlling the frequency in power systems with high renewable shares.**

Manuscript received April 22, 2021; revised July 27, 2021; accepted August 20, 2021. Date of publication August 24, 2021; date of current version February 2, 2022. The work of Hassan Haes Alhelou was supported in part by the Science Foundation Ireland (SFI) under the SFI Strategic Partnership Programme under Grant SFI/15/SPP/E3125 and in part by the UCD Energy Institute. Paper no. TII-21-1786. *(Corresponding author: Hassan Haes Alhelou.)*

Hassan Haes Alhelou is with the School of Electrical and Electronic Engineering, University College Dublin, Dublin 4, Ireland (e-mail: hassan.haesalhelou@ucd.ie).

Harish Parthasarathy is with the Department of Electronics and Communication Engineering, Netaji Subhas University of Technology, New Delhi 110078, India (e-mail: harishp@nsit.ac.in).

Neelu Nagpal is with the Department of Electrical and Electronics Engineering, Maharaja Agrasen Institute of Technology, New Delhi 110086, India (e-mail: nagpalneelu1971@ieee.org).

Vijyant Agarwal is with the Division of MPEA, Netaji Subhas University of Technology, New Delhi 110078, India (e-mail: vijaynt.agarwal@gmail.com).

Hardik Nagpal is with ZS Associates, Gurugram 122002, India (e-mail: nagpal.hardik5@gmail.com).

Pierluigi Siano is with the Department of Management and Innovation Systems, University of Salerno, 84084 Fisciano (Salerno), Italy, and also with the Department of Electrical and Electronic Engineering Science, University of Johannesburg, Johannesburg 2006, South Africa (e-mail: psiano@unisa.it).

Color versions of one or more figures in this article are available at https://doi.org/10.1109/TII.2021.3107396.

Digital Object Identifier 10.1109/TII.2021.3107396

***Index Terms*—Decentralized control, disturbance observer (DO), renewable energy, secondary control, smart grid, state estimation, stochastic system.**

## I. Introduction

### A. Motivation and Problem Statement

EACH area in an interconnected power system has responsibility to meet its own load requirements along with exchange of scheduled power among the adjoining areas as per energy market contracts. Violation of the generation-demand balance within a power area and/or contracted power exchange with other areas results in frequency deviation and power flow fluctuation through tie-lines [1], [2]. With the participation of renewable energy sources (RES), distributed generation, new types of load, and liberal energy markets, there is an increase of randomness and intermittent, especially in demand short-term profile and the power generated from RES, leading to a high stochastic characteristic of the system [3]–[5]. This affects the stability and security of interconnected modern power systems. This means that the modern power systems suffer from variation and stochastic sources in both the demand and generation sides, unlike conventional power systems, resulting in high frequency and power flow deviations and variations. These undesirable variations affect the operation, stability, and security in modern power systems and limit the penetration level of RES due to the fact that the increase of renewable energy share reduces the rotating inertia, which affects the frequency stability. The aforementioned issues highlight the problem statement that motivates research activities in frequency control, more specifically the secondary frequency control, which is also known as load frequency control (LFC).

### B. Literature Review

To achieve effective and robust LFC, many efforts have been made in recent years considering different power system models and control strategies [6]. This article focuses on frequency control in modern power systems based on observation and dynamic state estimation techniques. Due to space limitation, readers who are interested in other techniques applied to power system frequency control, can refer to adaptive controller [7],

sliding-mode controller [8], [9], intelligent controller [10], [11], optimal controller [12], or hybrid controller [13]. However, most of the aforementioned techniques have several technical and practical issues that limit their feasible implementation in reality, as highlighted in the recent comprehensive literature survey regarding the methods suggested for LFC in the conventional, and modern smart power systems [14]. Many of power systems around the globe still utilize conventional and the abovementioned control techniques, which clarify the reasons behind several of blackouts and power cuts in many power systems around the world due to frequency stability issues that highlight the need for new control methods that can handle the consequences of increasing the RES shares on power system frequency stability.

Control methods based on dynamic state estimation techniques have shown promising results for small-scale systems but the assumption of the availability of all states without corrupting with noise affects their implementation feasibility in large scale power systems [15]. Thus, there is a need to estimate the inaccessible or immeasurable states in order to overcome their implementation feasibility issues [16], [17]. For instance, in [18] and [19], the control signal has been dynamically generated by the observer, i.e., the error feedback to a controller is based on the observer output rather than the actual state incorporating noise. In power systems, functional observers have been designed to directly estimate the control signal rather than states for each area, which helps with reducing the dynamic order of the full-state observer [20].

In most of the existing literature, disturbance observer (DO) theory has been developed only for the constant disturbance [21], [22], but in practice, stochastic and time-varying [23] disturbances cannot be avoided due to internal and external different types of noises and disturbances [24]. In [25], it has been proven that a power system subjected to disturbance would be a time-varying and uncertain system. These uncertainties might be present in the form of plant modeling error, interconnection, nonlinearity, parameters, etc. The experimental investigations infer that frequency waveform has oscillations of small amplitude that accounts for randomness in the power system [26].

In [27], a new deterministic unknown input observer-based secondary frequency control method has been suggested for interconnected large scale power systems. The suggested method has the ability to convert the control structure to a fully decentralized one, but it cannot handle the random disturbances and noises, which limit their implementations. In [20], a functional observer has been proposed for LFC in power systems. Even the provided control structure is interesting and can reduce the order of the observer, it cannot provide a fully decentralized control structure and does not able to handle the variations from both demand and generation sides. Therefore, the aforementioned functional controller is not suitable for power systems with high shares of RES like modern power systems. In [28], for the first time, the DO has been developed for power system applications, more specifically for estimating the magnitude of the disturbance in power systems. However, the developed DO is applicable for protection applications in power systems, e.g., under frequency load shedding, and cannot control the frequency in modern systems since it needs a large disturbance, i.e., generating unit disconnection, to be able to estimate the power deficit, which highlights its infeasibility for secondary frequency control applications. In [29], a letter has suggested a two-layer active disturbance rejection control method with the compensation of estimated equivalent input disturbances for LFC of the multiarea interconnected power system. However, the suggested method requires a two-layer which increases its implementation complexity and does not able to handle random and stochastic variations from RES. Likewise, the suggested control structure does not guarantee a decentralized control for LFC, which brings technical and practical challenges. The aforementioned survey clearly shows the research gaps, and technical and practical issues related to frequency control that need to be well-investigated and addressed in order to enable high share of RES and mitigate the impacts of high stochasticity and intermittency in both demand and generation sides in modern power systems.

### C. Contribution

This article proposes a novel DO-based frequency control method for power systems with high renewable shares. It proposes a new algorithm for defining the time-varying random disturbance as one of the state variable. Unlike previous control method, a new computational technique is formulated in this article by first treating the total disturbance as a state, then tracking this disturbance and finally, rejecting this estimated disturbance. In the proposed control algorithm, most of the errors incurred in the desired variables are compensated through DO and remaining error is minimized by the controller to bring the actual output, i.e., maintaining the frequency in a desirable level. The proposed method is validated on a well-known system frequency response (SFR) benchmark for interconnected power systems with high RES shares. The results verified the superiority of the proposed control method over other techniques.

The main contributions of this article are as follows.

1) The proposal of a stochastic framework to present the system dynamics considering possible disturbances as one of the states. Furthermore, the model is modified and described as joint dynamics of states and the observer with desired state and observer error feedback.
2) The development of a new state observer to estimate the states of system including disturbance for anticipatory control and action in the presence of uncertain spin and spin free generation and load demand, which provides direction to the system operator to adjust the energy reserves to compensate with any disturbance incurred in the system after getting idea of its estimated value.
3) The decentralization of the proposed DO-based controller scheme.
4) Making the implementation of optimal controller based on dynamic estimators more feasible using any appropriate kind of state observers, not necessarily EKF.
5) The design of controller based on joint minimization of state trajectory tracking and state observer estimate error energies and has the ability to handle disturbances, noises, and time-delays.
6) Providing sensitivity, stability, and robustness analysis of the developed stochastic LFC model.

### D. Organization

The rest of this article is organized as follows. Section II provides the system dynamics and control methodology. The

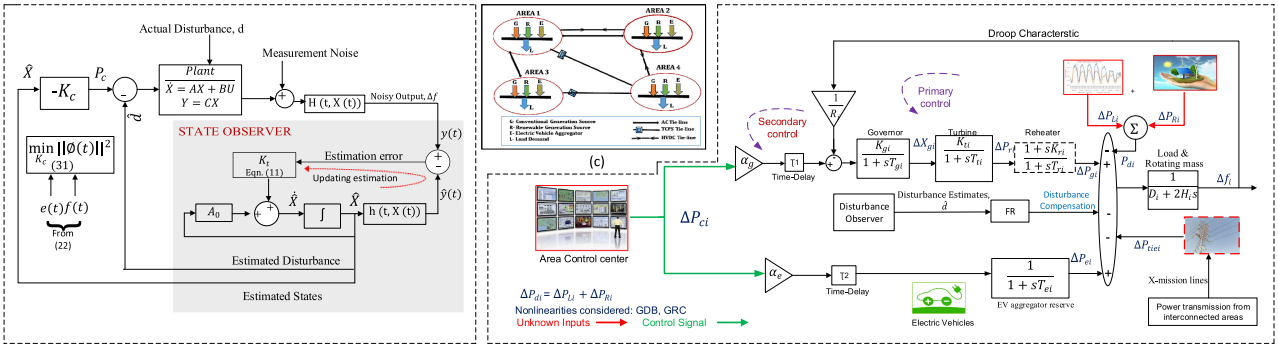


Fig. 1. (a) Block diagram of DOBC system. (b) Frequency response model of $i$th area of interconnected power system configuration under study. (c) Schematic diagram of interconnected four area power system.

observer is proposed in Section III, while Section IV proposes stochastic LFC. The sensitivity and robustness are studied in Section V. The benchmark, results, and findings are discussed in Sections VI–VIII. Finally, Section IX concludes this article.

## II. System Dynamics and Frequency Control Methodology

Let us consider an interconnected power system in which the frequency response model of $i$th area is depicted in Fig. 1(b). The $i$th area consists of an equivalent reheated thermal unit, an aggregated electric vehicle (EVs) unit representing their storage as a flexible demand, an uncontrolled input for modeling the variations of both electric demand and RES generation. The differential-algebraic equation of the $i$th is represented as

$$\left.\begin{aligned}
\Delta\dot{f}_i &= \tfrac{1}{2H_i}\Delta P_{ri} + \tfrac{1}{2H_i}\Delta P_{ei} - \tfrac{1}{2H_i}\Delta P_{di} \\
&\quad - \tfrac{D_i}{2H_i}\Delta f_i - \tfrac{1}{2H_i}\Delta P_{\text{tie}} - \Delta P_{\text{tie}} \\
\Delta\dot{P}_{gi} &= \tfrac{K_{ti}K_{ri}}{T_{ti}T_{ri}}\Delta X_{gi} + \tfrac{T_{ti}-K_{ri}}{T_{ti}T_{ri}}\Delta P_{ri} - \tfrac{1}{T_{ri}}\Delta P_{gi} \\
\Delta\dot{P}_{ri} &= \tfrac{K_{ti}}{T_{ti}}\Delta X_{gi} - \tfrac{1}{T_{ti}}\Delta P_{ri} \\
\Delta\dot{X}_{gi} &= -\tfrac{K_{gi}}{R_i T_{gi}}\Delta f_i - \tfrac{1}{T_{gi}}\Delta X_{gi} + \tfrac{K_{gi}\alpha_{gi}}{T_{gi}}\Delta P_{ci} \\
\Delta\dot{P}_{ei} &= -\tfrac{1}{T_{ei}}\Delta P_{ei} + \tfrac{}{T_{gi}}\Delta X_{gi} + \tfrac{K_{gi}\alpha_{gi}}{T_{gi}}\Delta P_{ci}
\end{aligned}\right\} \quad (1)$$

where $\Delta f-$ frequency variation, $\Delta P_g-$ output electrical power variation, $\Delta P_r-$ output mechanical power variation of the reheater, $\Delta X_g-$ Change in valve position, and $\Delta\dot{P}_e-$ output power variation of flexible loads, i.e., EVs in this article. $K_g$ and $T_g-$ the governor's gain and time constant, $K_r$ and $T_r-$ gain and time constant of the reheat section, $K_t$ and $T_t-$ gain and time constant the thermal turbine, and $K_e$ and $T_e-$ gain and time constant of the EV model. The main parameters of synchronous generator are inertia constant $H$, the damping coefficient $D$, and the speed droop $R$, respectively. In Fig. 1(b), the term FR refers to fast reserve sources that can help in preventing the frequency decline by releasing the active power reserve quickly.

The abovementioned description of the $i$th area is a generalized model of an area in an interconnected power systems with high RES shares consisting of several areas, where $i = 1, 2, \ldots, N$; $N$ is the number of connected areas. The model is a well-known benchmark for modeling power systems for frequency response and control studies, known as model, which is a sufficient model for designing and testing new frequency control methods [10], [14].

The variation in frequency, generated mechanical power, generated electrical power, storage power, and valve position are the nonrandom components of the system dynamics while $\Delta P_d$ and $\Delta P_{\text{tie}}$ along with other system uncertainties constitute to be random part with $\sigma dB_1$ as the noise component of the state.

It is evident that the system has to encounter various disturbances having both nonrandom and random parts. In a compact matrix form, the state dynamic model of the power system can be rewritten from (1) with the definitions for the state vector, input vector, and disturbance vector as

$$\left.\begin{aligned}
X_i &= [\Delta f_i \;\; \Delta X_{gi} \;\; \Delta P_{ri} \;\; \Delta P_{gi} \;\; \Delta P_{ei} \;\; d_i]^T \\
u_i &= [\Delta P_{ci}]; \quad d_i = [\Delta P_{di} \;\; \Delta P_{\text{tie},i} \;\; \delta_{ti}]
\end{aligned}\right\}. \quad (2)$$

It is assumed that the total disturbance of the system includes modeled or unmodeled disturbance. $\delta_t$ represents unmodeled disturbance that includes measurement, time-delay, estimation, and parameter uncertainty, in addition to randomness in the power deviation within and outside the area ($P_{di}$ and $P_{\text{tie}}$).

The requisite system (1) proposed as dynamic model including disturbance and noise as

$$\dot{X} = AX + BU + d + W_1; \quad Y(t) = CX + V_1 \quad (3)$$

where $X \in \mathbb{R}^{n\times 1}-$ state vector, $U \in \mathbb{R}^{r\times 1}-$ control input vector, $Y \in \mathbb{R}^{m\times 1}-$ output vector, and $d(t) \in \mathbb{R}^{q\times 1}-$ the disturbance vector. Also, $A-$ System matrix, $B-$Input matrix, $C-$output matrix, $d-$ nonrandom component disturbance, and $W_1$ is the random component of the disturbance present in the system.

The problem of LFC is more severe in case of interconnected power systems with low inertia due to high renewable shares than isolated power system. In multiarea power systems, connection between the power regains is done using tie-lines. These tie-lines can be ac power lines, HVdc links, and thyristor controlled phase shifters (TCPS) transmissions that transfer the scheduled power transfer between different areas [5]. Even in the event of a significant frequency deviation, each control area will retain its adjoining control areas interconnections, provided that the safe operation of its own system is not compromised. The aforementioned SFR model is a verified benchmark for frequency studies in modern power systems, which is widely adopted for verifying the recently suggested methods [27], [28], [36].

In this section, a sufficient model and its benchmark are introduced, which are necessary for designing and testing the proposed DO-based frequency control method in the following section. In order to introduce the proposed control method, it is crucial to list out the main assumptions and considerations that taken into account in this article, as follows.

1) The SFR model of interconnected power systems is adopted for designing and validating the proposed frequency control method.
2) To mimic reality and real-word power systems constraints, the adopted SFR model considers the nonlinearities, including governor dead-band (GDB) and generation rate constraint (GRC).
3) To consider modern power systems and future smart grids, it is assumed that the power system under investigation is with high penetration level of RES.
4) It is assumed that only few measurements, like real-world power systems, are available in the control center by wide-area monitoring system (WAMS) infrastructure, while other internal dynamic states need to be observed and handled by the proposed method.
5) The design of the proposed method considers the model uncertainties, and external disturbances.
6) It is assumed that the measured variables are accompanied noises that need to be handled, and assumed that the power system is subjected to variations from both demand and generation sides.

## III. Proposed DO

In this section, a state observer is devised to estimate the states of system, including disturbances. In (1), the deterministic dynamics of a system is presented considering state vector as $X$. Now, considering the total disturbance of the system (including random and nonrandom components) as one of the state, $d$ then, the requisite system proposed as dynamic model considering disturbances as one of the state as in (3). Now, the state equations can be rewritten as

$$\frac{dX}{dt} = AX + BU + d - \widehat{d} + \widehat{d} + W_1;\ \text{Assuming } d - \widehat{d} = W_2. \tag{4}$$

In this formation, the disturbance estimation error, $(d - \widehat{d})$ is regarded as a component of the process white noise [23]. randomness of the system dynamics is considered as $W_1 = \sigma \frac{dB_1}{dt} = \sigma I \dot{B}_1$ and its behavior can be treated as white Gaussian noise (WGN). Also, $W_2 = \sigma_2 I \frac{dB_2}{dt} = \sigma_2 I \dot{B}_2$ is assumed to be disturbance estimation error, can be treated as WGN, but the dynamics of $W_2$ is independent of $W_1$.

*Remark 1:* The construction of the DO is based upon the equation, $\frac{d\widehat{d}}{dt} = L(d - \widehat{d})$, where $L$ is a positive derivative matrix. The basic philosophy behind this equation is to increase $\widehat{d}$, if $\widehat{d} < d$ and decrease $\widehat{d}$, if $\widehat{d} > d$ and most of the DOs reported in the literature are based on this fundamental principle. The output of the DO may not be exact as its conventional design is based on the assumption that it is asymptotically a dc signal. Thus, in this work, disturbance estimation error is regarded as another white noise process. Furthermore, the DO output becomes another state variable, which will be recursively estimated by EKF yielding original system states and better estimated disturbance outputs

$$\text{Considering, } \frac{d\widehat{d}}{dt} \approx L(d - \widehat{d}) = LW_2 = \sigma_2 \frac{dB_2}{dt} \tag{5}$$

$$\text{Considering, } \frac{d\widehat{d}}{dt} \approx L(d - \widehat{d}) = LW_2 = \sigma_2 \frac{dB_2}{dt}. \tag{6}$$

The state dynamics of the observer is

$$\left.\begin{aligned}\begin{bmatrix}\dot{X}\\ \dot{\widehat{d}}\end{bmatrix} &= \begin{bmatrix}AX + BU + \widehat{d} + W_1 + W_2\\ LW_2\end{bmatrix}\\ &= \begin{bmatrix}AX + BU + \widehat{d}\\ 0\end{bmatrix} + \begin{bmatrix}I & I\\ 0 & L\end{bmatrix}\begin{bmatrix}W_1\\ W_2\end{bmatrix}\end{aligned}\right\}. \tag{7}$$

Furthermore, (7) can be rewritten as

$$\begin{bmatrix}\dot{X}\\ \dot{\widehat{d}}\end{bmatrix} = \begin{bmatrix}A & I\\ 0 & 0\end{bmatrix}\begin{bmatrix}X\\ \hat{d}\end{bmatrix} + \begin{bmatrix}B\\ 0\end{bmatrix}U + \begin{bmatrix}I & I\\ 0 & L\end{bmatrix} \times \begin{bmatrix}\sigma_1 I & 0\\ 0 & \sigma_2 I\end{bmatrix}\begin{bmatrix}\dot{B}_1\\ \dot{B}_2\end{bmatrix}. \tag{8}$$

The state dynamics (8) can be expressed as

$$\frac{d\xi}{dt} = A_0\xi + B_0 U + GR_w B_w \tag{9}$$

where $\xi = \begin{bmatrix}X\\ \widehat{d}\end{bmatrix}; A_0 = \begin{bmatrix}A & I\\ 0 & 0\end{bmatrix}; B_0 = \begin{bmatrix}B\\ 0\end{bmatrix}; G = \begin{bmatrix}I & I\\ 0 & L\end{bmatrix}$ $C = \begin{bmatrix}C_1 & 0\\ 0 & C_2\end{bmatrix}; R_w = \begin{bmatrix}\sigma_1 I & 0\\ 0 & \sigma_2 I\end{bmatrix}; B_w = \begin{bmatrix}\dot{B}_1\\ \dot{B}_2\end{bmatrix}$.

It should be noted that $B$ is a matrix while $B_1, B_2$ are vector valued Brownian motion processes, and hence, no confusion should arise in this context. The output vector is written as

$$y = HC\xi + V \tag{10}$$

where $y$ is the measured output vector, which may be corrupted by noise, $V$ and $H$ are the state observation matrix with value such that $HC = [1 \quad 0_{1\times 5}]$ and $HCX = \Delta f$.

EKF is used as state observer cum DO. The dynamics of the EKF for this study is developed as

$$\frac{d\widehat{\xi}}{dt} = A_0\widehat{\xi} + B_0 U + K_t(y - HC\widehat{\xi}). \tag{11}$$

The Kalman gain is defined as

$$K_t = (R_v)^{-1} P_t (HC)^T (HC) P_t \tag{12}$$

with measurement noise covariance, $R_v = \begin{bmatrix}\sigma_{v1}^2 & 0\\ 0 & \sigma_{v2}^2\end{bmatrix}$, the Riccatti equation for the state observer error covariance evolution considering $R = GR_w$ is

$$\frac{dP_t}{dt} = -P_t(HC)^T {R_v}^{-1} HCP_t + A_0 P_t + P_t A_0^T + RR^T. \tag{13}$$

### A. Computation of "L"

In order to attain robust and accurate estimation results, it is required to obtain the value of $L$. Although in the literature, its value has been considered as unity [18] but here the proposed

state observer design computes the value of $L$ with the help of the following derivation:

$$\left.\begin{array}{l} \frac{dd(t)}{dt}=0;\ \frac{(\widehat{d}(t)+\delta\widehat{d}(t))-\widehat{d}(t)}{dt}\approx\frac{d\widehat{d}(t)}{dt}=L(d(t)-\widehat{d}(t)) \\ \dot{\widehat{d}}(t)=L(\dot{X}-AX-BU-W-\widehat{d}) \\ \text{If } \frac{d\widehat{d}}{dt}=L(d-\widehat{d}) \text{ then, } \widehat{d}(t)=e^{-tL}\widehat{d}(0)+\int_0^t e^{-\tau L}Ld(\tau)d\tau \end{array}\right\}. \tag{14}$$

*Remark 2:* If we consider, $\widehat{d}=Z+P(X)$ then, $\frac{dZ}{dt}+P'(X)\dot{X}=\frac{d\widehat{d}}{dt}=L(\dot{X}-AX-BU-\widehat{d})$ and, $P'(X)=L$, $\frac{dZ}{dt}=-L(AX+BU+\widehat{d})$. This construction of the DO ensures that the dynamics of the disturbance estimate at a given time depends only on the current state and not on its time derivative. This is plausible because while computing the time derivative of the state, large spikes can arise causing breakdown of the DO. Based on the idea that after a sufficient long time $T$, the disturbance estimation error norm should be a small fraction of its initial value and further, the disturbance estimate should have a smaller rate of change, approximate lower and upper bounds on the DO coefficient matrix $L$ can be derived by obtaining estimates for its largest and smallest eigen values. The derivation of eigen values can be as follows:

$$\widehat{d}(t)=e^{tL}\widehat{d}(0)+\int_0^t e^{(t-\tau)L}Ld(\tau)d\tau. \tag{15}$$

Neglecting the initial condition, and using the fact that $d(t)$ is asymptotically a dc signal

$$\left.\begin{array}{l} \widehat{d}(t)=\int_{-\infty}^t e^{-(t-\tau)L}Ld(\tau)d\tau \\ d(t)-\widehat{d}(t)=\epsilon(t) \text{ and } \frac{d\epsilon}{dt}\approx-\frac{d\widehat{d}}{dt} \\ \qquad\qquad =-L\epsilon(t) \text{ or the expression for} \\ \epsilon(t)=e^{-tL}\epsilon(0) \text{ and } \mathbb{E}[||\epsilon(t)||^2=\sigma_\epsilon^2(0)\text{Tr}[e^{-tL}e^{-tLT}] \end{array}\right\}. \tag{16}$$

It is known that the value of $L$ lies between predicted range of the eigen values, i.e., L must be large to make $e^{-tLT}$ small since

$$\epsilon(t)=d(t)-\widehat{d}(t)\approx\ e^{-tT}\epsilon(0);\epsilon(T)=e^{-tLT}\epsilon(0). \tag{17}$$

The choice of $T$ is large enough such that $d(t)$ for $t\geq T$ is nearly a dc signal. Consider, $\mathbb{E}[||\epsilon(t)||$ is small and equal to

$$\left.\begin{array}{l} \mathbb{E}[||\epsilon(t)||=\frac{\alpha}{100} \\ \text{Furthermore, } \frac{||\epsilon(T)||}{||\epsilon(0)||}\leq||e^{-LT}||\leq\exp(-T_{\min}]Re\lambda_k) \\ \qquad\qquad \leq\frac{\alpha}{100}\leq r \\ \Rightarrow\lambda_{\min}^R\geq\frac{1}{T}\ln\frac{100}{\alpha} \end{array}\right\}. \tag{18}$$

As $\frac{d\widehat{d}}{dt}=L(d-\widehat{d})$ and for $t\geq T$; $\frac{d\widehat{d}}{dt}|_T\approx r$; $d(T)-\widehat{d}(T)=e^{-TL}(d(0-\widehat{d}(0))||d(T)-\widehat{d}(T)||\leq||e^{-TL}(d(0)-\widehat{d}(0))||$. This results

$$||L||\leq\frac{r}{||d(0)||||e^{-TL}||} \text{ and } \lambda_{\max}^R\leq\frac{r}{||d(0)||e^{-T\lambda_{\min}^R}}. \tag{19}$$

We can write $L=GI$ where $\lambda_{\min}^R\leq G\leq\lambda_{\max}^R$. After getting $L$ correctly for estimated disturbance, the resultant disturbance is neutralized with the system disturbance. Although in (4), it is assumed that there is always a perpetual estimation error, $W_2$ including components of state disturbance and frequency variations but, it also keeps on diminishing by the action of EKF. In this section, the aim of the DO is to estimate the disturbances and uncertainties as exogenous inputs and considered these as estimated total disturbance $\widehat{d}$. In the following section, a state feedback controller is developed taking observer into account to get noise free system states available to the state feedback controller.

## IV. DO-Based Controller

An optimal controller is designed based on the minimization of joint state estimation and state tracking error energies for each area of the power systems. But prior to feeding the states to controller, the compensation of system total disturbance $d$ by the estimated disturbance $\widehat{d}$ is done, as shown in Fig. 1(a). Thus, the proposed DOBC is based on the estimation of $\widehat{d}$, which is rejected, and afterward the remaining estimated states, $\widehat{X}$ are used as to form decentralized optimal state feedback LFC for the system, as shown in Fig. 1(b).

From the system dynamics (1), it is seen that the state variable equations are linear and first order in time. However, not all the state variables are directly observable and only a small subset of linear combination of the stochastic states (with measurement noise) can be observed. This observation is called the true system output, $y(t)$. Also, the desired system output without noise is denoted by $y_d(t)$. The aim is to remove stochasticity so that the true system output is as close as possible to the desired system output. Since only the noisy output trajectory is measurable where EKF is used to estimate the states using this measured output. Furthermore, a state error feedback to the input of the system is provided with the corresponding matrix feedback coefficient designed on the basis of a block processing approach. The proposed control algorithm for a system is formulated in such a way that the mean square value of the sum of the state estimation error and the state trajectory tracking error over a given time duration is a minimum. Here, the state feedback error is computed as the difference between the desired state trajectory and the EKF-based state trajectories, i.e., $\xi_d(t)$–$\widehat{\xi}(t)$. This mean square error value is calculated in terms of the output error feedback control matrix (that influences the state dynamics) and its expression is simplified using the eigen-decomposition of the resulting modified state dynamical matrix. Finally, the control law that yields the optimal feedback coefficient matrix is obtained by solving this optimization problem involving minimizing a function of the eigen values and eigen vectors of the modified state dynamical matrix.

Refer Fig. 1(a), a structure of state feedback controller is described with the controller input based on the error between state observer and the desired state after compensating the estimated disturbance using (9) and (10) prior to controller action. Thus, state dynamics of the system with controller considering estimated states (from observer) takes the form

$$\frac{d\xi}{dt}=A_0\xi+B_0U+G\sum_w B_w+K_c(C(\xi_d-\widehat{\xi}). \tag{20}$$

Furthermore, the Ricatti equation for the estimated states is formulated as

$$\frac{d\widehat{\xi}}{dt}=A_0\xi+B_0U+K_t(HC\xi+V-HC\widehat{\xi}). \tag{21}$$

These equations will be used to compute the mean square trajectory tracking and state observer error values over a prescribed time duration and, hence, designing the controller to minimize the combination of these two error energies. The state tracking error, $f(t)$ and state observer error, $e(t)$ are expressed as follows:

$$f(t) = \xi_d - \widehat{\xi};\ e(t) = \xi - \widehat{\xi}. \tag{22}$$

The reference state dynamics (i.e., the original plant model without noise) is represented as following:

$$\frac{d\xi_d}{dt} = A_0\xi_d + B_0U. \tag{23}$$

The error dynamics can be represented as

$$\left.\begin{aligned}\tfrac{de}{dt} &= (A_0 - K_tHC)e + K_cCf + GR_wB_w - K_tV\\ \tfrac{df}{dt} &= A_0f - K_tHCe - K_tV\end{aligned}\right\} \tag{24}$$

$$\frac{d}{dt}\begin{bmatrix}f(t)\\ e(t)\end{bmatrix} = \begin{bmatrix}A_0 & -K_tHC\\ \tilde{K}_cC & A_0 - K_tHC\end{bmatrix}\begin{bmatrix}f\\ e\end{bmatrix} + \begin{bmatrix}0 & -K_t\\ I & -K_t\end{bmatrix}\begin{bmatrix}GR_wB_w\\ V\end{bmatrix} \tag{25}$$

Let, $\Phi(t) = \begin{bmatrix}f(t)\\ e(t)\end{bmatrix}$; $\widetilde{A}(K_c) = \begin{bmatrix}A_0 & -K_tHC\\ K_cC & A_0 - K_tHC\end{bmatrix}$ $Q_t = \begin{bmatrix}0 & -K_t\\ I & -K_t\end{bmatrix}$; $V = R_vB_v$.

Now (25) can be rewritten as a single joint error dynamics

$$\frac{d\Phi(t)}{dt} = \widetilde{A}(K_c)\Phi(t) + Q_t\begin{bmatrix}GR_WB_w\\ R_vB_v\end{bmatrix}. \tag{26}$$

When steady state is reached, matrix $K_t = K_\infty = K$ and (12) becomes constant given by

$$K = R_v^{-1}P_\infty(HC)^T(HC)P_\infty \tag{27}$$

where $P_\infty$ saturates the algebraic Riccati equation as

$$A_0P_\infty + P_\infty A_0^T + GG^T - \sigma_v^{-2}P_\infty(HC)(HC)^TP_\infty. \tag{28}$$

Substituting $K_t = K$, controller gain $K_c$ must be chosen so that all eigen values of

$$\widetilde{A}(K_c) = \begin{bmatrix}A_0 & -KHC\\ K_cC & A_0 - KHC\end{bmatrix}$$

have negative real parts for stability. The solution of (26) for large $t$, is

$$\Phi(t) = \int_0^t e^{(t-\tau)\widetilde{A}(K_c)}Q_\tau\begin{bmatrix}GR_wB_w\\ R_vB_v\end{bmatrix}d\tau. \tag{29}$$

The output observer estimation error relative to the desire signal, i.e., tracking error based on observer estimate of the state feedback using a controller gain matrix into the state variable dynamics. Thus, an attempt to derive the linearized stochastic dynamics for the joint evolution of state estimation and state tracking error is made keeping in view that the states considered here also contains the disturbance estimate as a part. This error evolution equation contains controller gain as a matrix parameter

$$\mathbb{E}[||\Phi(t)||^2dt] = \int_0^t \mathbb{E}\{\Phi(t)\Phi(t)^T\}dt. \tag{30}$$

The optimal design of the controller gain matrix is achieved by minimizing the trace of this joint error covariance matrix (30) w.r.t controller gain $K_c$

$$\min_{K_c}\left\{\mathrm{Tr}\int_0^T dt\int_0^t e^{t-\tau\widetilde{A}(K_c)}Q_\tau\begin{bmatrix}GR_w & 0\\ 0 & R_v\end{bmatrix} Q_\tau^Te^{t-\tau}\widetilde{A}(K_c)^Td\tau\right\}. \tag{31}$$

*Remark 3*: Let $\widetilde{A}(K_c) = \sum_{j=1}^p \lambda_j(K_c)u_j(K_c)v_j(K_c)^T$ be the eigen decomposition of $\widetilde{A}(K_c)$, thus, $v_j^Tu_k = \delta_jk, 1 \le j,k \le p$ and $\sum_{j=1}^p u_jv_j^T = I_p$. Let, $M = Q_s\begin{bmatrix}GR_w & 0\\ 0 & R_v\end{bmatrix}Q_s^T$ then

$$\mathrm{Tr}\left(\int_0^t \mathbb{E}\{\Phi(t)\Phi(t)^T\}dt\right) = \int_0^T \mathrm{Tr}\left(e^{(T-s)\widehat{A}(K_c)}Me^{(T-s)\widehat{A}(K_c)^T}ds\right). \tag{32}$$

We can further express (32) as

$$\int_0^T \mathrm{Tr}(e^{(T-s)\sum_{j,l=1}^p\lambda_j(K_c)u_j(K_c)v_j(K_c)^T}Me^{(T-s)}$$

$$\sum_{j,l=1}^p \lambda_l(K_c)v_m(K_c)u_m(K_c).^Tds) = \sum_{j,l=1}\frac{[F_1][F_2-1]}{F_3}$$

$$\text{where } F_1 = \sum_{j,l=1}[v_j(K_c)^TMv_m(K_c)u_m(K_c)^Tu_j(K_c)$$

$$F_2 = [v_j(K_c)^TMv_m(K_c)u_m(K_c)^Tu_j(K_c)]$$

$$F_3 = [\lambda_j(K_c) + \lambda_l(K_c)]. \tag{33}$$

Expression (33) is minimized w.r.t. $K_c$. Thus, the proposed DOBC is based on the estimation of $\widehat{d}$, which is rejected, and afterward the remaining estimated states, $\widehat{X}$ are used as to form decentralized optimal state feedback LFC for system shown in Fig. 1(b).

The performance of the proposed DOBC is superior as the controller is designed based on minimization of a combination of all kinds of error energies of state estimate, disturbance estimate, and state tracking. Furthermore, using the expression of the joint error energies, sensitivity of system w.r.t. parameters fluctuations is carried out in the following section.

## V. On the Sensitivity, Robustness, and Stability

### A. Sensitivity and Robustness Analysis

In this section, it is demonstrated via computations how to calculate the changes in the state observer error variance under small changes in the system parameters. This calculation helps to investigate the robustness of proposed state cum disturbance observer while the previous derivations regarding controller design support the stochastic stability of proposed estimation and tracking algorithm. Let $\theta$ denotes the fluctuations in parameters and it is intended to analysis the robustness and sensitivity of the plant output fluctuations against $\theta$. The system matrix can be represented

as $A_0 = A_0(\theta) = A_{00} + \sum_{k=1}^{p} \theta_k A_{0k}$ and $\theta \sim \left(\frac{1}{H_i}, \frac{D_i}{H_1}, \frac{K_{ti}K_{ri}}{T_{ti}T_{ri}}, \frac{T_{ti}-K_{ri}}{T_{ti}T_{ri}}, \frac{1}{T_{ri}}, \frac{Kti}{T_{ti}}, \frac{K_{gi}}{R_i T_{gi}}, \frac{1}{T_{gi}}, \frac{K_{gi}\alpha_{gi}}{T_{gi}}\right)$. The following points are to be noted.

(i) If $\theta$ fluctuates to $\theta + \delta\theta$, then the amount by which $P_\infty = P$ and $K_\infty = K$ change will be denoted as $P \longrightarrow P + \delta P$ and $K \longrightarrow K + \delta K$. The change in state observer error variance, $P$ can be denoted by Tr$[\delta P]$

$$\left.\begin{array}{l} \delta P = \sum_{k=1}^{p} \frac{\partial P}{\partial \theta_k}\delta\theta_k + \frac{1}{2}\sum_{k,m=1}^{p} \frac{\delta^2 P}{\delta\theta_k \delta\theta_m}\delta\theta_k\delta\theta_m \\ \text{If} < \delta\theta_k >= 0, < \delta\theta_k\delta\theta_m >= \rho_\theta(k,m) \\ \text{Tr} < \delta P > \approx \frac{1}{2}\sum_{n,m=1}^{p} \frac{\delta^2 P}{\delta\theta_k \delta_m}\rho_\theta(k,m) = \frac{1}{2}\text{Tr}\{\rho_\theta \ \nabla_\theta^T \ \nabla_\theta \ P\} \end{array}\right\}. \tag{34}$$

(ii) Change in $\mathbb{E}[||f(t)||^2 + \lambda||e(t)||^2]$ as $t \to \infty$ is termed as weighting of average of state tracking and observer error energies w.r.t. $\delta\theta$

$$\left.\begin{array}{l} \frac{d}{dt}\begin{bmatrix} f(t) \\ e(t) \end{bmatrix} \\ = \begin{bmatrix} A_{00} + \sum_{k=1}^{p}\theta_k A_{0k} & -KHC \\ \tilde{K}_c C & A_{00} + \sum_{k=1}^{p}\theta_k A_{0k} - KHC \end{bmatrix} \\ \quad \begin{bmatrix} f(t) \\ e(t) \end{bmatrix} + \begin{bmatrix} -KV_t \\ GW_t - KV_t \end{bmatrix} \\ = [A_0(0) + \sum_{k=1}^{p}\theta_k A_{0k}(1)]\begin{bmatrix} f(t) \\ e(t) \end{bmatrix} + S_t \begin{bmatrix} W_t \\ V_t \end{bmatrix} \\ = I_2 \otimes A_{ok}, \ 1 \le k \le p \\ \text{where } A_0(0) = \begin{bmatrix} A_{00} & -KHC \\ K_c C & A_{00} - KHC \end{bmatrix}; S_t = \begin{bmatrix} 0 & -K \\ G & -K \end{bmatrix} \end{array}\right\}. \tag{35}$$

The updated solution of (35) is given as

$$\begin{bmatrix} f(t) \\ e(t) \end{bmatrix} = \int_0^t e^{(t-\tau)(A_0(0) + \sum_{k=1}^{p}\theta_k A_{0k}(1))} S_t \begin{bmatrix} W_\tau \\ V_\tau \end{bmatrix} d\tau. \tag{36}$$

Thus, Tr $< \delta P > \approx \frac{1}{2}\sum_{k,m=1}^{p} \frac{\partial^2}{\partial\theta_k\theta_m}\rho_\theta(k,m)$

$$\left.\begin{array}{l} \approx \int_0^T \left[ e^{\tau(A(0) + \sum_j \theta_j A_j(1))} S_t \begin{bmatrix} \sigma_w^2 & 0 \\ 0 & \sigma_v^2 \end{bmatrix} \right. \\ \left. S_t^T e^{\tau(A(0)^T + \sum_j \theta_j A_j(1)^T)} \right] d\tau \end{array}\right\}. \tag{37}$$

From basic Lie-algebra theory (differential of the exponential [32], [33]), the following expressions are presented

$$\left.\begin{array}{l} \exp(t(A_0 + \sum \theta_k A_k(1))) = \exp(tA(0)) + \exp(tA(0)) \\ \left(\frac{I - e^{(-tadA(0)))}}{adA(0))}\right)(\sum \theta_k A(1))) + O(||\theta||^2)e^{(t(A_0))} \\ [I + \sum \theta_k g(tad(A(0))((A_k(1)))] + O(||\theta||^2) \\ \text{where } g(z) = \frac{1-e^{-z}}{z} = \sum_{n=0}^{\infty}\frac{z^n(-1)^n}{n+1!} \end{array}\right\}.$$

Thus, the change in the error process caused by small parameter fluctuations is given by $\begin{bmatrix} \delta f(t) \\ \delta e(t) \end{bmatrix}$ and the joint error process is

$$\begin{bmatrix} \delta f(t) \\ \delta e(t) \end{bmatrix} = \int_0^t \exp((t-\tau)A(0)\sum \theta_k g((t-\tau)ad\ (A(0)) \times (A_k(1))S \begin{bmatrix} W(\tau) \\ V(\tau)) \end{bmatrix} d\tau \tag{38}$$

In that case,

$$\begin{array}{l} \mathbb{E}[||\delta f(t)^2 + \lambda||\delta e(t)||^2] = \mathbb{E}\left\{ \begin{bmatrix} \delta f(t) \\ \delta e(t) \end{bmatrix}^T Q \begin{bmatrix} \delta f(t) \\ \delta e(t) \end{bmatrix} \right\} \\ = \text{Tr}[Q\mathbb{E}\begin{bmatrix} \delta f(t) \\ \delta e(t) \end{bmatrix}[\delta f(t) \ \delta e(t)]^T \mathbb{E}\left\{\begin{bmatrix} \delta f(t) \\ \delta e(t) \end{bmatrix}[\delta f(t)^T \ \delta e(t)^T\right\} \\ = \int_0^t \left\{ e^{(\tau A(0))} \sum_k \theta_k g(\tau \ ad \ A(0))(A_k(1))SR_0S^T \right. \\ \left. \sum_m \theta_m (g(\tau \ adA(0))(A_m(1))^T e^{(\tau A(0)^T)} \right\} d\tau \\ \text{where } R_0\delta(t-\tau) = \mathbb{E}\left\{\begin{bmatrix} W(t) \\ V(t) \end{bmatrix}[W(t)^T \quad V(t)^T]\right\}. \end{array} \tag{39}$$

The following equation determines the final correlation function of the shift in the trajectory tracking and state estimation error taking the DO into account when the parameters of the system undergo small fluctuations

$$\begin{array}{l} \delta R_{fe}(t) = \sum_{k,m=1}^{p} \theta_k\theta_m \int_0^t e^{(\tau A(0))} g(\tau \ adA(0))(A_k(1))S \\ R_0.S^T g(\tau \ adA(0))(A_k(1))^T d\tau. \end{array} \tag{40}$$

Finally, (40) can be used to assess the robustness of the system because the error fluctuation energy has been expressed as a quadratic form in the parameter fluctuations.

*Remark 4:* The proposed algorithm is robust w.r.t. parameter fluctuations because a linear in parameters model has been chosen, i.e., the plant matrix $A(\theta) = A_0 + \sum_{k=1}^{p}\theta_k A_k$ is linear in parameters $\theta_k$. If it is, for example, quadratic in the parameters $\theta_k$, i.e., of form $A(\theta) = A_0 + \sum_{k=1}^{p}\theta_k A_k(1) + \sum_{k=1}^{p}\theta_k\theta_m A_{km}(2)$ the sensitivity of the tracking and observer error energies to parameter fluctuation will be much larger. However, in such cases, $\theta_k(1) = \theta_k$ as our parameters are $\theta_{k,m} =< \theta_k\theta_m >$ ($< \cdot >$ denotes ensemble average of a random parameter). Thus, the linear quadratic in parameter (LQIP) model becomes Linear in parameter (LIP). Then, the error energies would be less sensitive to parameter fluctuations.

### B. Stability Analysis

To guarantee the stability, the eigenvalues of the controlled matrix, i.e., $\tilde{A}(K_c) = \begin{pmatrix} A_0 & -KHC \\ K_c C & A_0 - KHC \end{pmatrix}$, should have negative real parts. Applying calculations to the above $2 \times 2$ block structured matrix [34], one would have that eigenvalues of $\tilde{A}(K_c)$ are the roots of the equation which are, $\det(A_0 - \lambda.I).\det(A_0 - KHC - \lambda.I + K_c C(A_0 - \lambda.I)^{-1}KHC) = 0$.

In the presence of control, $K_c \neq 0$, these are precisely the root of $\det(A_0 - KHC - \lambda.I + K_c C(A_0 - \lambda.I)^{-1}KHC) = 0$, while in the absence of control ($K_c = 0$), these are the union of the roots of $\det(A_0 - \lambda.I) = 0$ and of $\det(A_0 - KHC -$

$\lambda.I) = 0$, i.e., set of eigenvalues of $A_0$ and of $A_0 - KHC$. In case there is a computing complexity to find the exact roots of the aforementioned characteristic equation, a perturbation theoretic approach can be adopted as given as follows.

Let us suppose that an eigenvalue $\lambda$ of the uncontrolled system (i.e., $K_c = 0$) is only slightly displaced toward the right half $s$-plane. Then, a small controller gain $K_c$ may be designed so that the perturbed eigenvalue $\lambda + \delta\lambda$ falls in the left half $s$-plane. This design is achieved using the following description.

With $B(\lambda) = \tilde{A}(K_c) - \lambda.I$, one would have $\det(\tilde{A}(K_c) - (\lambda + \delta\lambda).I) = \det(B(\lambda)(I - \delta\lambda.B(\lambda)^{-1})) = \det(B(\lambda))(1 - \delta\lambda.\mathrm{Tr}(B(\lambda)^{-1}) + O(\delta\lambda^2))$. Setting this to zero gives, $\delta\lambda = 1/\mathrm{Tr}(B(\lambda)^{-1})$, which shows that $K_c$ can be adjusted so that the shift $\delta\lambda$ in $\lambda$ is such that the resulting eigenvalue $\lambda + \delta\lambda$ falls in the left half $s$-plane.

It is to note that if $\lambda$ is not an eigenvalue of either $A_0$ or of $A_0 - KHC$, then $B(\lambda) = \tilde{A}(K_c) - \lambda.I = B(0) + B(1)$, where $B(0) = \tilde{A}(0) - \lambda.I = \begin{pmatrix} A_0 - \lambda.I & -KHC \\ 0 & A_0 - KHC - \lambda.I \end{pmatrix}$ and $B(1) = \begin{pmatrix} 0 & 0 \\ K_cC & 0 \end{pmatrix}$. Since $K_c$ is assumed to be small in norm, $B(1)$ is small. Then, $B(\lambda)^{-1} = B(0)^{-1} - B(0)^{-1}B(1)B(0)^{-1} + O(\| K_c \|^2)$, so, $\det(\tilde{A}(K_c) - (\lambda + \delta\lambda)I) = 0$ gives for small $K_c$ that $\delta\lambda = 1/\mathrm{Tr}(B(\lambda)^{-1}) = 1/(\mathrm{Tr}(B(0)^{-1} - \mathrm{Tr}(B(0)^{-2}B(1))))$ approximately and from this equation, it is simple to calculate $K_c$ so that the shift $\delta\lambda$ is as per our requirements. In fact writing $K_c = \beta(1)K_c(1) + \cdots + \beta(q)K_c(q)$ where $\beta(1), \ldots, \beta(q)$ are adjustable parameters and writing $B(1, m) = \begin{pmatrix} 0 & 0 \\ K_c(m)C & 0 \end{pmatrix}, m = 1, 2, \ldots, q$, we have $\mathrm{Tr}(B(0)^{-2}B(1)) = \sum_{m=1}^{q} \beta(m)\mathrm{Tr}(B(0)^{-2}B(1, m))$ so the abovementioned equation may be expressed as, $\mathrm{Tr}(B(0)^{-1}) - \sum_{m=1}^{q} \beta(m)\mathrm{Tr}(B(0)^{-2}B(1, m)) = 1/\delta\lambda$, which is a linear problem for calculating the $\beta(m)'s$.

An alternate method for calculating the shift in the eigenvalues when the controller is introduced is via perturbation theory for eigenvalues of diagonable matrices. Writing the diagonalization of $\tilde{A}(0)$ as $\tilde{A}(0) = \sum_a \lambda(a)u_a v_a^T, v_a^T u_b = \delta_{ab}$. We use standard first-order eigenvalue perturbation theory to get the following perturbations in the eigenvalue on the introduction of the perturbation term $B(1)$ assuming $K_c$, and hence, $B(1)$ to be small; $\tilde{A}(K_c) = \tilde{A}(0) + B(1)$, and $\delta\lambda_a = v_a^T B(1)u_a$. Since this is a linear form in $K_c$, $K_c$ can be easily determined for appropriate placement of $\delta\lambda_a$.

## VI. Benchmark and Power System Under Consideration

To validate the proposed method in the previous sections, a verified benchmark based on the SFR model is adopted, where its sufficiency for designing and testing secondary frequency controllers has been widely discussed and confirmed in the literature [36]. The number of the connected areas is consider to be four, i.e., $N = 4$. The dynamics of each area, $i$th area are given in Section II, as descried in (1–3), while Fig. 1(b) shows the block diagram that represents the dynamics of the $i$th area.

To clearly show the structure of the areas connection and the type of the used tie-lines for connecting the different areas, the topology of the system benchmark is depicted in Fig. 2. This benchmark is widely used in the literature where its full data is available in [36] and [27]. Likewise, the necessary data for

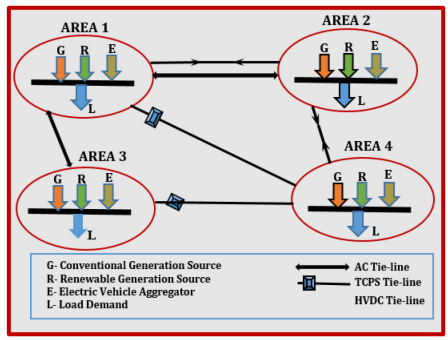


Fig. 2. Schematic diagram of the interconnected four area power system.

redoing the simulation is given in the Appendix. As mentioned previously, the adopted system is considered to have high share of RES, as shown in Fig. 2. To consider the recent trends in modern power systems toward smart grid concept, the demand side is considered to provide a part of the required secondary reserve by electric vehicles as depicted in Figs. 1(b) and 2.

## VII. Simulation Results and Analysis

An extensive simulation study is done to investigate the performance of the proposed decentralized LFC based on DOBC for power systems. DOBC is developed for a generalized $N$-area interconnected power systems, but to demonstrate its performance through simulations, a topology of interconnected four-area system is considered. Initially, MATLAB script and simulink model are developed for the system under investigation and for obtaining the observer matrices and gains. The study takes into account different types of disturbances and operation scenarios of power systems. After successful implementation of the proposed decentralized DOBC approach on a single area, individual areas are joined using variety of tie-lines and the performance of interconnected system is also investigated. A computational model is developed with the help of aforementioned linearized state space matrix (1) and values of physical parameters are substituted using [27]. The states of the system include unknown total disturbance $d$. The matrix form of (1) is considered to represent the stochastic model (incorporating the system disturbance) of a power system for the simulations. EKF is used as state observer for estimating six states, i.e., $\widehat{X} = [\Delta\widehat{f}\ \ \Delta\widehat{X_g}\ \ \Delta\widehat{P_r}\ \ \Delta\widehat{P_g}\ \ \Delta\widehat{P_e}\ \ \widehat{d}]^T$. The following expression of EKF is used as Riccati equation for the feedback and the error covariance. The model of state observer (8) is developed using the dynamics as follows:

$$\left.\begin{aligned} &\dot{\widehat{X}} = A\hat{X} + PH^T\sigma_v^{-1}(\dot{Z} - \Delta f) \\ &\dot{P} = A_0P_t + P_tA_0^T - \sigma_v^{-2}P_t(HC)^T(HC)P_t + GG^T \\ &\sigma_v = \begin{bmatrix} \mathrm{Cov.}(w) & 0 \\ 0 & \mathrm{Cov.}(w) \end{bmatrix};\ G = \begin{bmatrix} I & 0 \\ 0 & I \end{bmatrix} \\ &\text{For the present measurement linear system} \\ &\dot{Z} = HX + \sigma_v dV = \Delta f \text{ where } H = \begin{bmatrix} I & 0 \\ 0 & I \end{bmatrix} \end{aligned}\right\}. \quad (41)$$

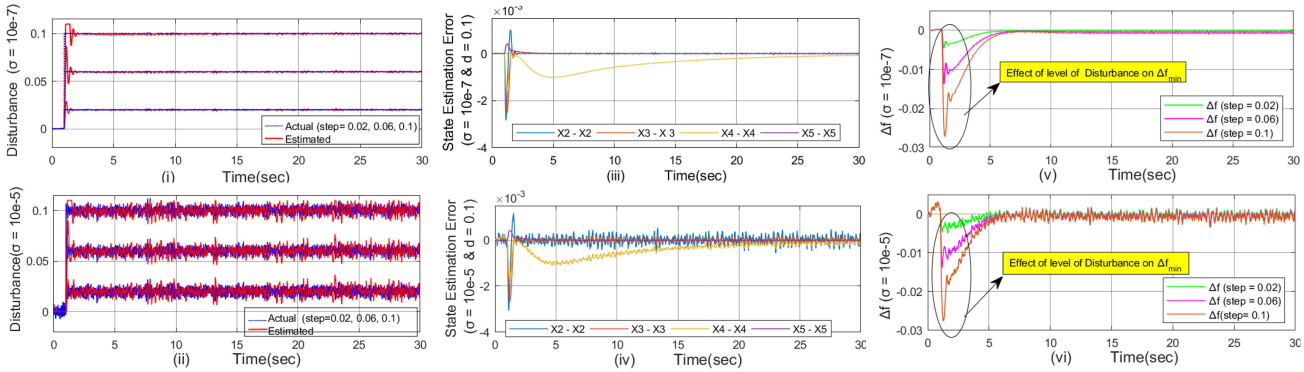


Fig. 3. Simulation results: Disturbance estimation ($\widehat{d}$) with varying nonrandom disturbances, (i) at Cov.$10^{-7}$, (ii) at Cov. $10^{-5}$; State estimation error, (iii) at Cov.$10^{-7}$, (iv) at Cov. $10^{-5}$; Frequency deviation, (v) at Cov.$10^{-7}$, and (vi) at Cov.$10^{-5}$.

In what follows, the control and dynamic performance is investigated by several scenarios in order to verify the superiority of the proposed method.

### A. Performance of the Proposed State Observer

The accuracy of estimation performed by the EKF under the effect of disturbances for different scenarios given in Table I is shown in Fig. 3. Table I describes the different levels of step disturbance (nonrandom) and stochastic disturbance considered for the simulations. These simulations are done considering that the participation of EV reserve is set to 10%, i.e., ($K_e = 0.1$ and $K_g = 0.9$) with delay time ($\tau_{d2}$) 0.05 s. From Fig. 3(i) and (ii), it is evident that the state observer is capable to estimate the actual disturbance. The accuracy of the observer is further verified by the convergence of estimation errors of states as shown in Fig. 3(iii) and (iv), which verify the superiority of the proposed technique. Also, the results depict the frequency deviation for different types of the considered disturbances and noises, as shown in Fig. 3(v) and (vi).

TABLE I
LEVEL OF RANDOM AND NONRANDOM DISTURBANCE CONSIDERED AND EFFECT ON $\Delta f_{\text{MIN}}$

| Step disturbance | Cov. $10^{-7}$ | | Cov. $10^{-5}$ | |
|---|---|---|---|---|
| Level | $t$ | $\Delta f_{min}$ | $t$ | $\Delta f_{min}$ |
| 0.02 | 1.19 | -0.004493 | 1.17 | -0.004672 |
| 0.06 | 1.17 | -0.01371 | 1.17 | -0.01385 |
| 0.1 | 1.26 | 0.02720 | 1.26 | -0.02778 |

TABLE II
EFFECT OF VARIATION OF SYSTEM PARAMETERS ON THE PERFORMANCE OF PROPOSED DOBC SYSTEM

| Variation of System Parameters → | | |
|---|---|---|
| % Change in $T_g$ and $T_t$ or $T_e$ | $\Delta f_{min}$ (for $\Delta T_g$ and $\Delta T_t$) | $\Delta f_{min}$ (for $\Delta T_e$) |
| +60, -60 | -0.02739, -0.02798 | -0.02765, -0.02772 |
| +40, -40 | -0.02731, -0.02781 | -0.02753, -0.02743 |
| +20, -20 | -0.02728, -0.02771 | -0.02738, -0.02719 |
| 0 | -0.02720 | -0.02720 |

### B. Performance of the Proposed DOBC Scheme for Isolated and Interconnected Power Systems

The simulation study is done both for the single-area power system and interconnected four-area power system to investigate the performance of the proposed control scheme under the influence of system disturbances and uncertainties like load disturbance, time delays, and system parameters. The corresponding results of control area 1 are presented in Fig. 4. Table I presents different scenarios to observe the effect of DOBC on frequency deviation for first-control area.

The simulation results in Table II present the effect of power system parameters uncertainties on frequency deviation. Furthermore, tests are performed to observe the effects of contribution of EV reserve power, ($P_e$) on the frequency deviation considering sudden change in $\Delta P_e$ due to cyber or physic attack or problems in the infrastructure. The results are summarized in Fig. 4(vi), which shows the brilliant perform ace of the proposed method in considering technical and practical challenges.

Furthermore, investigation is carried out to ensure the robustness of the proposed scheme under the influence of time-delay present in the communication channel. The aforementioned tests to observe the frequency deviation with the change in the parameters are done considering a 0.1 magnitude of step disturbance and $10^{-7}$ covariance value for the noise. Fig. 4(i) depicts that frequency Nadir (FN) ($\Delta f_{\text{min}}$) gets affected with the change in the random disturbance but proposed DOBC has the capability to tackle this stochasticity in the system and control the frequency deviation ($\Delta f$). Furthermore, a remarkable improvement in the oscillations from higher and lower side of the frequency deviation response along with quick settling time (ST) (before 5 s) approves the good performance of the control approach. In Table I, $\Delta f_{\text{min}}$ is noted for different scenarios with corresponding time. With the increase of the level of disturbance, the frequency deviation is increasing but still it is less than that of maximum permissible limit after employing DOBC to the system. When the system is under the influence of stochastic disturbance, it is quite interesting to see the effect of disturbance compensation before feeding the estimated states to controller in Fig. 4(iii). The dynamics of the system has higher overshoots and undershoots and also the response gets settled within 30 s.

The proposed controller is robust with respect to the system parameter changes and able to maintain the safe dynamic response as indicated in graphs Fig. 4(iv)–(vi) and Table II. The

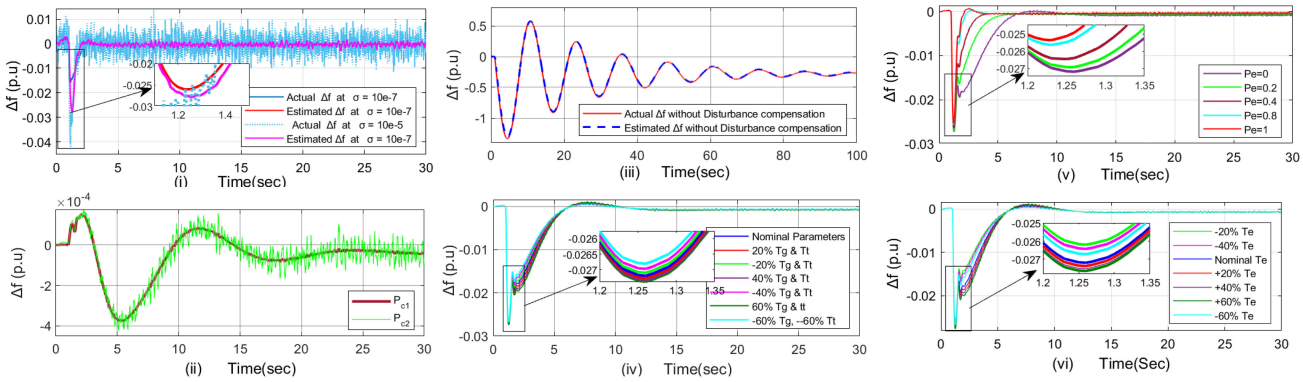


Fig. 4. Simulation results: Investigation of proposed DOBC scheme on frequency deviation ($\Delta f$). (i) Effect of change in random disturbance. (ii) Effect of change in random disturbance on controller output. (iii) Effect of noncompensating disturbance before controller action. (iv) Effect of change in system parameters of turbine and governor. (v) Effect of EV reserve contribution. (vi) Effect of change in system parameters of EV aggregate system.

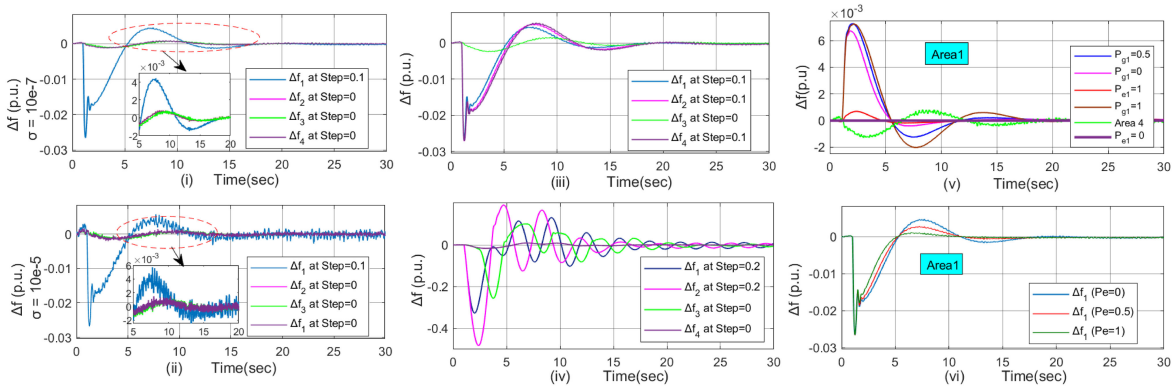


Fig. 5. Simulation results: Investigation of proposed DOBC scheme on frequency deviation of interconnected areas $\Delta f$ (i) and (ii) Case $A_{11}$: Effect of change in random disturbance; (iii) Case $B_{11}$; (iv) Case $E_{11}$; (iv) Case $A_{11}$: Effect on $P_g$ and $P_e$ with change in EV reserve contribution; (v) Case $A_{11}$: Effect of change in EV reserve contribution.

time to occur $\Delta f_{\min}$ is same, i.e., 1.26 s in every case but the value of $\Delta f_{\min}$ is different for every % change in the time constants viz. $T_g$ and $T_t$ or $T_e$. The effect of contribution of EV reserved is observed in Fig. 4(vi), indicating that with the change in the contribution of EV reserve power to system, the dynamic response gets affected but the frequency response is preserved by the proposed control method. The robustness of proposed control scheme under several test scenarios for single area supports that in case of a power system is in island mode, the dynamic response under the influence of uncertainty is not compromised. There is no significant effect on the frequency deviation considering different amount of time delays (0.05–2 s in $\tau_1$ and $\tau_2$). This ensures the robustness of the proposed method in this article against uncertain time delay in the system. After validating the performance of DOBC for the first area power system, the simulation study is extended for the four-area interconnected power system. These individual areas are connected using tie-lines of different types as shown in the schematic diagram [refer Fig. 1(c)] of a typical power system. The details of these lines and their data have been referred from [20]. Simulations are conducted to check the performance of DOBC for the combined four area systems considering various load scenarios in different areas [refer Table III]. The corresponding results are displayed in Fig. 5. Fig. 5(i) and (ii) (refer Case $A_{11}$) depicts that increase in step disturbance along with the randomness (in terms covariance, $\sigma$) of Area 1 affects the $\Delta f$ response of all areas but the proposed approach can successfully in settle the responses of Area1–Area4 with 10 s. Fig. 5(iii) and (iv) represents the results of severe situations, which a power system may undergo. The results confirm that the proposed control approach is a success as frequency deviation in both cases settle to zero within prescribed time. Furthermore, Fig. 5(v) presents the smooth response of power deviations, with the variable contribution of both conventional and EV reserves. This is a good indication of better life time of governor, thus, assures a good performance of the proposed control strategy for the multiarea multisource interconnected power systems. While monitoring the frequency response with the variable EV reserve contribution in Fig. 5(vi), the proposed DOBC scheme approves its robustness against participation of flexible demand with an effective dynamic response. The aforementioned simulation results confirm that the proposed control approach has brilliant performance and can handle different types of disturbances and uncertainties. The aforementioned results and discussions verify the robustness and superiority of the proposed control method. It is confirmed that the proposed control method has the ability

TABLE III
DIFFERENT DISTURBANCE SCENARIOS OF INTERCONNECTED FOUR-AREA SYSTEMS CONSIDERED

| Variation of load disturbance (Step) in different areas → | | | | |
|---|---|---|---|---|
| Case | Area 1 | Area 2 | Area 3 | Area 4 |
| $A_{11}$ | 0.1 | - | - | - |
| $B_{11}$ | 0.1 | 0.1 | - | - |
| $C_{11}$ | 0.1 | 0.1 | - | 0.1 |
| $D_{11}$ | 0.1 | 0.1 | 0.1 | 0.1 |
| $E_{11}$ | 0.2 | 0.2 | - | - |

TABLE IV
COMPARISON OF PROPOSED DOBC WITH OTHER METHODS, CONSIDERING TECHNICAL ISSUES

| Method | Topology | DT | ST [S.] | FN [Hz] |
|---|---|---|---|---|
| [35] | Centralized | Step | 150 | 0.09 |
| [27] | Quasi-decentralized | Step | 60 | 0.03 |
| [36] | Distributed | Step | 13 | 0.05 |
| Proposed | Decentralized | Step + Random | 8 | 0.02 |

to handle practical and technical issues related to the frequency control in modern power systems.

Table IV compares the results of the proposed method against other most recent and relevant methods in the literature. It is clear that the proposed method provides a fully decentralized control structure for controlling an interconnected power systems, while others cannot provide a such effective solution. For instance, a centralized control method has been proposed in [35], where the control complexity would increase by increasing the number of areas, which limits its implementation capability in comparison with the proposed method in this article. Likewise, a distributed controller has been suggested in [36], which requires a remote signals to be transferred from other areas to each area under control, where missing a such signal leads to instability issues. Therefore, the proposed method is this article suggests the best control topology in comparing to other methods in the literature that used dynamic state estimation methods for LFC.

Table IV shows that all other methods in the literature consider only one type of disturbance (DT), i.e., step disturbance, while the proposed method in this article considers both step and random disturbance, which mimics the reality as the disturbance in real-world power systems is a random one. In fact, most of the other methods cannot handle random disturbances leading to instability issues or at least to undesirable dynamic performance. This fact gives a superiority to the proposed method in this article over other techniques.

In case of ST and the FN after a specific disturbance, the comparative study shows that the proposed method has a better performance over other techniques. The aforementioned results confirm the superiority of the proposed method, as well as its capability and feasibility for implementation in modern power systems with high share of RES.

## VIII. NECESSITIES, FINDINGS, AND ADVANTAGES

This article focuses on secondary frequency control in interconnected power systems with high RES share. As aforementioned, increasing the penetration level of RES results in reducing the total rotating inertia, which affect the frequency stability and security in modern power systems. On the other hand, the increase of RES share has brought new variation source to the operation of power systems due to the RES intermittency and stochasticity. In the conventional power systems, the source of variations was the demand side only, while it has become the both demand and generation sides, which brings new challenges to frequency control in modern power systems. Therefore, it has been highlighted that there is a need for new control methods based on the disturbance estimation that considers both step and random types of disturbances in modeling the SFR. Likewise, converting conventional control topology and structures toward fully decentralized control structure is one of the necessities that motivates recent research activities in the topic of modern power system frequency control.

The main findings obtained from this research output include the following.

1) The ability of the proposed method to accurately tracking the disturbance and rejecting it in order to improve the dynamic performance of the frequency controller.
2) The potential to handle uncertainties, which is verified theoretically during the design of the observer-based frequency controller and confirmed by a several simulation scenarios.
3) The ability to take into account different DT including random disturbance coming from both demand and generation sides.
4) The proposed secondary frequency controller has a better performance in comparison with other methods and can handle technical and practical issues.
5) Brilliant performance of the proposed observer-based secondary frequency control method, which has a less ST and a lower FN that makes it suitable for modern power systems with higher variations and disturbance magnitudes.

In addition to the previous main findings, the proposed method has the advantage of controlling the frequency in a power system with diverse transmission links including ac power transmission lines, HVdc transmission links, and TCPS transmissions as verified by the considered power system under investigation in this article. Likewise, the proposed method can coordinate and manage the secondary reserve from both generation and demand sides, where the contribution of electric vehicles is taken into account in this article.

## IX. CONCLUSION

This article suggests a DO-based controller for power system frequency applications. A state observer is successfully developed to estimate the system states considering practical challenges of system without any extra computational cost. In the proposed DOBC approach, the time-varying random and nonrandom disturbance were first estimated and then neutralized. The results have shown accurate estimation as DOB has produced a new state $(\hat{d})$ and then residual noise of estimation. The proposed algorithm has successfully been implemented for a generalized controller of an LFC based on observer derived state error feedback. The convergence of estimation errors of states approves the capability of the proposed state observer. It is found that the proposed method is capable to tolerate fluctuations in the part of the system without exceeding predefined tolerance bounds in the vicinity of some nominal dynamic behavior. Additionally, the quality of control action is maintained for a

wider range of operation with more robustness as compared to some existing control approaches. Thus, it is concluded that proposed DOBC-based LFC has the potential to resolve the concerns related to constant and stochastic disturbances, which may include load fluctuations, uncertainties of renewable resources and system parameters, energy reserves, and time delay effectively. The main findings in this article prove the applicability of the proposed method to be adopted for real-world power systems since it takes practical and technical challenges into account. As a future work, the proposed method can be developed for controlling other variables in power systems such as the voltage. Likewise, it can be adopted for controlling the frequency in microgrids in addition to interconnected power systems.

## APPENDIX

*Appendix A:* The power system data used in the simulation study is as follows [27], [36], [37].

$T_{ti} = 0.3,\ T_{gi} = 0.08,\ T_{ri} = 10,\ T_{ei} = 1,\ T_{s,ij} = 0.1,$ $T_{dc,i} = 0.2, T_{ji} = T_{ij} = 0.026, K_{gi} = 1, K_{ri} = 1, K_{ij} = 0.1,$ $D_i = 0.0083,\ H_i = 0.08335,\ M_i = 0.1667,\ K_{s,ij} = 1,\ b_i =$ $0.425,\ R_i = 2.40,\ {}_{g,i} = 0.9,\ {}_{e,i} = 0.1,$ and the nonlinearities including GRC and GDB are modeled based on [10], [36], [37].

*Appendix B:* To study the effect of random change in the disturbance on the mean square error in the state tracking and state estimation errors, one can rewrite (25) as

$$d\Phi(t)/dt = F_1\eta(t) + F_2 w(t)$$

where $w(t)$ is a white noise vector, which contains the disturbance estimation error $d(t) - \hat{d}(t)$ as a component. The components of $\Phi(t)$ are the state tracking error and state estimation error. In the general case, $w(t)$ may even be a correlated noise process. By solving the abovementioned differential equation, one obtains

$$\Phi(t) = \int_0^t \exp(t-\tau)F_1)F_2 w(\tau)d\tau.$$

Hence, the mean square error is

$$\mathbb{E} \parallel \Phi(t) \parallel^2 = \mathrm{Tr} \int_0^t \int_0^t \exp((t-\tau_1)F_1)F_2 R_{ww}(\tau_1,\tau_2)F_2^T \cdot\exp((t-\tau_2)F_1^T)d\tau_1 d\tau_2.$$

In case the disturbance statistics changes, it would induce a change in the statistics of $w(t)$, which would perturb its autocorrelation matrix from $R_{ww}(\tau_1,\tau_2)$ to $R_{ww}(\tau_1,\tau_2) + \delta R_{ww}(\tau_1,\tau_2)$. The corresponding change in the mean square tracking plus state estimation error would be given by

$$\delta\mathbb{E} \parallel \Phi(t) \parallel^2 = \int_0^t \int_0^t \mathrm{Tr}(\exp((t-\tau_1)F_1)F_2\delta R_{ww}(\tau_1,\tau_2)F_2^T \times \exp((t-\tau_2)F_1^T)d\tau_1 d\tau_2.$$

Now write down the KL expansion of the noise correlation as

$$R_{ww}(\tau_1,\tau_2) = \sum_i \lambda_i \phi_i(\tau_1)\phi_i(\tau_2)^T.$$

Then, from first-order perturbation theory for the eigenvalue problem for Hermitian operators, the perturbation in the noise correlation is given by

$$\delta R_{ww}(\tau_1,\tau_2) = \sum_i \delta\lambda_i.\phi_i(\tau_1)\phi_i(\tau_2)^T + \sum_i \lambda_i(\delta\phi_i(\tau_1).\phi_i(\tau_2)^T + \phi_i(\tau_1)\delta\phi_i(\tau_2)^T)$$

where the eigenvalue and eigenfunction perturbations are given by

$$\delta\lambda_i = <\phi_i|\delta R_{ww}|\phi_i> = \int\int \phi_i(\tau_1)^T .\delta R_{ww}(\tau_1,\tau_2)\phi_i(\tau_2)d\tau_1 d\tau_2$$

and $\delta\phi_i(\tau) = \sum_{j\neq i} \frac{\phi_j(\tau)<\phi_j|\delta R_{ww}|\phi_i>}{\lambda_i-\lambda_j}$.

Then, in terms of these eigen-perturbations, the change in the mean square error is

$$\delta\mathbb{E} \parallel \Phi(t) \parallel^2 = \sum_i \delta\lambda_i \int_0^t \int_0^t \phi_i(\tau_2)^T F_2^T \exp((t-\tau_2)F_1^T) .\exp((t-\tau_1)F_1)F_2.\phi_i(\tau_1)d\tau_1 d\tau_2 + 2\sum_i \lambda_i \int_0^t \int_0^t \phi_i(\tau_2)^T F_2^T \exp((t-\tau_2)F_1^T) .\exp((t-\tau_1)F_1)F_2\delta\phi_i(\tau_1)d\tau_1 d\tau_2.$$

The effect of change in random disturbance in the proposed work has been shown in Section VI using different simulation scenarios.

## ACKNOWLEDGMENT

The opinions, findings, and conclusions or recommendations expressed in this material are those of the authors and do not necessarily reflect the views of the Science Foundation Ireland.

## REFERENCES

[1] P. Siano, "Demand response and smart grids—A survey," *Renewable Sustain. Energy Rev.*, vol. 30, pp. 461–478, 2014.

[2] C. Chen, M. Cui, F. Li, S. Yin, and X. Wang, "Model-free emergency frequency control based on reinforcement learning," *IEEE Trans. Ind. Informat.*, vol. 17, no. 4, pp. 2336–2346, Apr. 2021.

[3] X.-C. Shangguan *et al.*, "Robust load frequency control for power system considering transmission delay and sampling period," *IEEE Trans. Ind. Informat.*, vol. 17, no. 8, pp. 5292–5303, Aug. 2021.

[4] J. Shukla, B. K. Panigrahi, and P. K. Ray, "Stochastic reconfiguration of distribution system considering stability, correlated loads and renewable energy based DGs with varying penetration," *Sustain. Energy, Grids Netw.*, vol. 23, 2020, Art no. 100366.

[5] T. N. Pham, H. Trinh, and L. V. Hien, "Load frequency control of power systems with electric vehicles and diverse transmission links using distributed functional observers," *IEEE Trans. Smart Grid*, vol. 7, no. 1, pp. 238–252, Jan. 2016.

[6] M. Kheshti, L. Ding, W. Bao, M. Yin, Q. Wu, and V. Terzija, "Toward intelligent inertial frequency participation of wind farms for the grid frequency control," *IEEE Trans. Ind. Informat.*, vol. 16, no. 11, pp. 6772–6786, Nov. 2020.

[7] T. H. Mohamed, M.-A. M-Alaminb, and A. M. Hassa "A novel adaptive load frequency control in single and interconnected power systems," *Ain Shams Eng. J.*, vol. 12, no. 2, pp. 1763–1773, 2020.

[8] Y. Mi, Y. Fu, C. Wang, and P. Wang, "Decentralized sliding mode load frequency control for multi-area power systems," *IEEE Trans. Power Syst.*, vol. 28, no. 4, pp. 4301–4309, Nov. 2013.

[9] S. Prasad, S. Purwar, and N. Kishor, "Non-linear sliding mode load frequency control in multi-area power system," *Control Eng. Pract.*, vol. 61, pp. 81–92, 2017.
[10] H. Bevrani and T. Hiyama, *Intelligent Automatic Generation Control*. Boca Raton, FL, USA: CRC Press, 2011.
[11] Y. Arya and N. Kumar, "BFOA-scaled fractional order fuzzy PID controller applied to AGC of multi-area multi-source electric power generating systems," *Swarm Evol.*, vol. 32, pp. 202–218, 2017.
[12] W. Su, H. Eichi, W. Zeng, and M.-Y. Chow, "A survey on the electrification of transportation in a smart grid environment," *IEEE Trans. Ind. Informat.*, vol. 8, no. 1, pp. 1–10, Feb. 2012.
[13] S. Kayalvizhi and D. M. Vinod Kumar, "Load frequency control of an isolated micro grid using fuzzy adaptive model predictive control," *IEEE Access*, vol. 5, pp. 16241–16251, 2020.
[14] H. Alhelou, M.-E. Hamedani-Golshan, R. Zamani, E. Heydarian-Forushani, and P. Siano, "Challenges and Opportunities of load frequency control in conventional, modern and future smart power systems: A comprehensive review," *Energies*, vol. 11, no. 10, 2018, Art no. 2497.
[15] Y.-H. Moon, H.S. Ryu, J.-G. Lee, and S. Kim, "Power system load frequency control using noise-tolerable PID feedback," in *Proc. IEEE Int. Symp. Ind. Electron. Proc.*, Pusan, South Korea, 2001, pp. 1714–1718.
[16] R. Abe, H. Taoka, and D. McQuilkin, "Digital grid: Communicative electrical grids of the future," *IEEE Trans. Smart Grid*, vol. 2, no. 2, pp. 399–410, Jun. 2011.
[17] A. Abbaspour, A. Sargolzaei, P. Forouzannezhad, K. K. Yen, and A. I. Sarwat, "Resilient control design for load frequency control system under false data injection attacks," *IEEE Trans. Ind. Electron.*, vol. 67, no. 9, pp. 7951–7962, Sep. 2020.
[18] F. Liu, Y. Li, Y. Cao, J. She, and M. Wu, "A two-layer active disturbance rejection controller design for load frequency control of interconnected power system," *IEEE Trans. Power Syst.*, vol. 31, no. 4, pp. 3320–3321, Jul. 2016.
[19] N. Nagpal, V. Agarwal, and B. Bhushan, "A real-time state-observer-based controller for a stochastic robotic manipulator," *IEEE Trans. Ind. Appl.*, vol. 54, no. 2, pp. 1806–1822, Mar./Apr. 2018.
[20] H. H. Alhelou, M. E. H. Golshan, and N. D. Hatziargyriou, "A decentralized functional observer based optimal LFC considering unknown inputs, uncertainties, and cyber-attacks," *IEEE Trans. Power Syst.*, vol. 34, no. 6, pp. 4408–4417, Nov. 2019.
[21] K. P. S. Parmar, S. Majhi, and D. P. Kothari, "Load frequency control of a realistic power system with multi-source power generation," *Elect. Power Energy Syst.*, vol. 42, pp. 426–433, 2012.
[22] S. Doolla and T. S. Bhatti, "Load frequency control of an isolated small-hydro power plant with reduced dump load," *IEEE Trans. Power Syst.*, vol. 21, no. 4, pp. 1912–1919, Nov. 2006.
[23] V. Agarwal and H. Parthasarathy, "Disturbance estimator as a state observer with extended Kalman filter for robotic manipulator," *Nonlinear Dyn.*, vol. 85, pp. 2809–2825, 2016.
[24] S. Li, J. Yang, W.-H. Chen, and X. Chen, *Disturbance Observer-Based Control: Methods and Applications*, 1st ed. Boca Raton, FL, USA: CRC Press, 2014. [Online]. Available: https://doi.org/10.1201/b16570.
[25] P. Kundur *et al.*, "Definition and classification of power system stability IEEE/CIGRE joint task force on stability terms and definitions," *IEEE Trans. Power Syst.*, vol. 19, no. 3, pp. 1387–1401, Aug. 2004.
[26] G. Benysek, J. Bojarski, R. Smolenski, M. Jarnut, and S. Werminski, "Application of stochastic decentralized active demand response (DADR) system for load frequency control," *IEEE Trans. Smart Grid*, vol. 9, no. 2, pp. 1055–1062, Mar. 2018.
[27] H. H. Alhelou, M. E. H. Golshan, and N. D. Hatziargyriou, "Deterministic dynamic state estimation-based optimal LFC for interconnected power systems using unknown input observer," *IEEE Trans. Smart Grid*, vol. 11, no. 2, pp. 1582–1592, Mar. 2020.
[28] H. H. Alhelou, M. H. Golshan, T. Njenda, and P. Siano, "WAMS-based online disturbance estimation in interconnected power systems using disturbance observer," *Appl. Sci.*, vol. 9, no. 5, p. 990, 2019.
[29] F. Liu, Y. Li, Y. Cao, J. She, and M. Wu, "A two-layer active disturbance rejection controller design for load frequency control of interconnected power system," *IEEE Trans. Power Syst.*, vol. 31, no. 4, pp. 3320–3321, Jul. 2016.
[30] W. Tan, "Unified tuning of PID load frequency controller for power systems via IMC," *IEEE Trans. Power Syst.*, vol. 25, no. 1, pp. 341–0350, Feb. 2010.
[31] K. Jagatheesan, B. Anand, N. Dey, and A.S. Ashour, "Artificial intelligence in performance analysis of load frequency control in thermal-wind-hydro power systems," *Int. J. Adv. Comput. Sci. Appl.*, vol. 6, pp. 203–212, 2015.
[32] M. K. Hanawal and R. Sundaresan, "Guessing revisited: A large deviations approach," *IEEE Trans. Inf. Theory*, vol. 57, no. 1, pp. 70–78, Jan. 2011.
[33] A. Dembo and O. Zeitouni, *Large Deviations Techniques and Applications—Stochastic Modelling and Applied Probability*, vol. 38. Berlin, Germany: Springer, 2009, doi: 10.1007/978-3-642-03311-73.
[34] C. Rao *et al.*, *Linear Statistical Inference and Its Applications*, vol. 2. New York, NY, USA:Wiley, 1973.
[35] D. Sharma and S. Mishra, "Non-linear disturbance observer-based improved frequency and tie-line power control of modern interconnected power systems," *IET Gener., Transmiss. Distrib.*, vol. 13, no. 16, pp. 3564–3573, 2020.
[36] T. N. Pham, H. Trinh, and L. V. Hien, "Load frequency control of power systems with electric vehicles and diverse transmission links using distributed functional observers," *IEEE Trans. Smart Grid*, vol. 7, no. 1, pp. 238–252, Jan. 2016.
[37] H. Haes and P. Cuffe, "A dynamic state estimator based tolerance control method against cyberattack and erroneous measured data for power systems," *IEEE Trans. Ind. Informat.*, to be published, doi: 10.1109/TII.2021.3093836.